The Mechanisms Underlying Colour Afterimages

Christoph Witzel, cwitzel@daad-alumni.de, School of Psychology, Southampton

Abstract. Negative colour afterimages are a fundamental phenomenon reflecting the adaptative mechanisms of colour processing. Despite its fundamental importance, the precise mechanisms underlying afterimages are very much controversial. What has been overlooked is that the adaptation of different mechanisms makes fundamentally different predictions about the hue and saturation of afterimages. We developed two experimental paradigms to measure the exact colours perceived in afterimages and test those predictions empirically. All results of these two different paradigms confirm that afterimages do not align with cone-opponency but instead tightly follow a well-founded, straight-forward model of cone adaptation (i.e., cone contrasts). This model implements cone adaptation according to Weber's Law, which is a direct consequence of the proportional decrement of photon catches due to cone bleaching and results in a nonlinear, multiplicative inverse function of cone excitations. This nonlinear adaptation of the three cones predicts three peaks of afterimage intensity that correspond with the three peaks of saturation and the three clusters of hue in the measurements of afterimages. Our findings establish cone-adaptation as the sole origin of negative colour afterimages. The quantitative cone-contrast model resolves apparent contradictions and provides a comprehensive, straight-forward explanation of the adaptive mechanisms underlying colour afterimages.

Keywords. After-effects, Colour Vision, Perceptual Adaptation, Perceptual Mechanisms, Visual Processing

Summary / Introduction

Negative colour afterimages are illusory colour experiences that occur after fixating and adapting to a coloured area for a sustained time[1]. Such afterimages are textbook examples of the most fundamental properties of human colour perception: chromatic adaptation, opponency, and dependence on context and beholder[2-6]. The adaptation underlying the induction of afterimages has been attributed to different mechanisms at all stages of the visual hierarchy. The classical explanation suggested afterimages are due to cone-bleaching at the first stage of colour processing[7], but others found contradictory results[8,9]. Most state-of-the-art research attributes afterimages to the cone-opponent mechanisms at the second stage of colour processing[2,5,10-12], but again others found contradictory results[13-15]. Still others, claim that afterimages occur through adaptation of higher, cortical mechanisms that involve shape and object recognition[16-18], binocular integration[19,20] and/or colour constancy[21], contradicting classical evidence for a retinal origin[22,23]. Here, we show unequivocal evidence that afterimages originate from cone adaptation at the first level of processing. Using two new paradigms, we measured the precise hue and saturation of afterimages for a wide range of inducers. We quantitatively model cone bleaching and adaptation through Weber fractions (cone contrasts)[24,25]. Results demonstrate that the quantitative cone-adaptation model completely predicts the colours induced in afterimages.

Results

Research and textbooks have missed the fact that the adaptation of different perceptual mechanisms makes fundamentally different predictions about the hue and saturation of afterimages[2-6,14,26]. These predictions can be tested empirically, using experimental paradigms that allow for measuring the exact colours perceived in afterimages. We developed two such paradigms, a fixed-location and a chaser-like simultaneous matching task (Figure 1.a & e).

Fixed-location Task. The first task combined a typical afterimage display with simultaneous matching (Figure 1.a). Observers simultaneously matched the hue of comparison stimuli with the hue of an afterimage that appears at the location of an inducing colour after that inducing colour disappeared. Chroma of comparison stimuli was kept constant (see Method). If afterimages strictly corresponded to cone-opponency their hues would be equally distributed along a circle because inducers were sampled from such a circle (the coloured circle in Figure 1.b,d). If there was non-linear adaptation to cone-opponency or any other kind of colour opponency (e.g., Hering colours), hues should align with the four directions of the respective two opponent dimensions. None of this was the case. Instead, observers' matches showed that the hues of afterimages were systematically shifted away from the cone-opponent hue directions (Figure 1.c) towards three directions that coarsely coincided with the directions of maximal cone excitations (Figure 1.d). To make precise predictions, we modelled cone adaptation through cone-contrasts (red line in Figure 1.b). The deviations of the measured afterimages from cone-opponency were strongly correlated with such deviations of the afterimages as simulated by cone-contrasts ($r(22) = .81$, $p < .001$; Figure 1-c). To simulate a hue histogram, we added response noise (black dots in Figure 1.b) to obtain a smooth probability distribution (black curve in Figure 1.d). This cone-adaptation model predicted the frequencies of hue selections with a correlation of over $r(70) = .62$, $p < .001$, across the 72 response hues. The distribution of responses for 24 inducers across 72 response options

produced artefact variation (zigzags in the grey area of Figure 1.c) that undermines a correlation with the probability distribution from the model. Smoothening the variation across the 72 response hues (red curve in Figure 1.d) counteracts those artifacts and yielded a correlation with the model of $r(70) = .80$, $p < .001$. These effects on hue selection were specific to afterimages, and did not occur in a control task, in which observers matched real colours in an otherwise same stimulus display (see supplementary material XXXX).

Chaser-Like Task. The model also makes predictions about the strength, i.e., the chroma, of the aftereffects (Figure 1.b). We used a chaser-like task (Figure 1.e) to maintain the afterimage over time, allowing for adjustments of both, hue and chroma, to match the induced colours without decay of afterimage strength over time. The average adjustments across 72 inducers (red curve in Figure 1.e) closely followed the predictions by the cone-adaptation model (grey area in Figure 1.e), resulting in a correlation of $r(70) = .90$, $p < .001$, between predicted and measured chroma. As in the other task, deviations from opponent hues were correlated between simulated and measured afterimages ($r(70) = .84$, $p < .001$, Figure 1.g), and the hue histogram for measured and modelled afterimages were strongly correlated, too ($r(70) = .81$, $p < .001$; cf. Figure 1.h). These results could also be produced at the individual level: For each of the 10 observers, there was a correlation between predicted and measured chroma ($r(70) = .43$ to $.87$, all $p < .001$); and for 9 out of 10 there was a positive correlation between measured and simulated deviations from opponent colours ($r(70) = .31$ to $.89$, all $p < .01$, except: $r(70) = 0.22$, $p = .07$) and between measured and simulated hue histograms ($r(70) = .28$ to $.61$, all $p < .05$; except: $r(70) = .19$, $p = .10$). The strength of afterimage induction through yellowish inducers and the shift of the corresponding afterimages away from cone-opponent blue towards the purplish S-cone direction are so pronounced that they are obvious to first-person experience (see attached animated image for illustration: the colour in the centre would be blue according to cone-opponency but is actually purple).

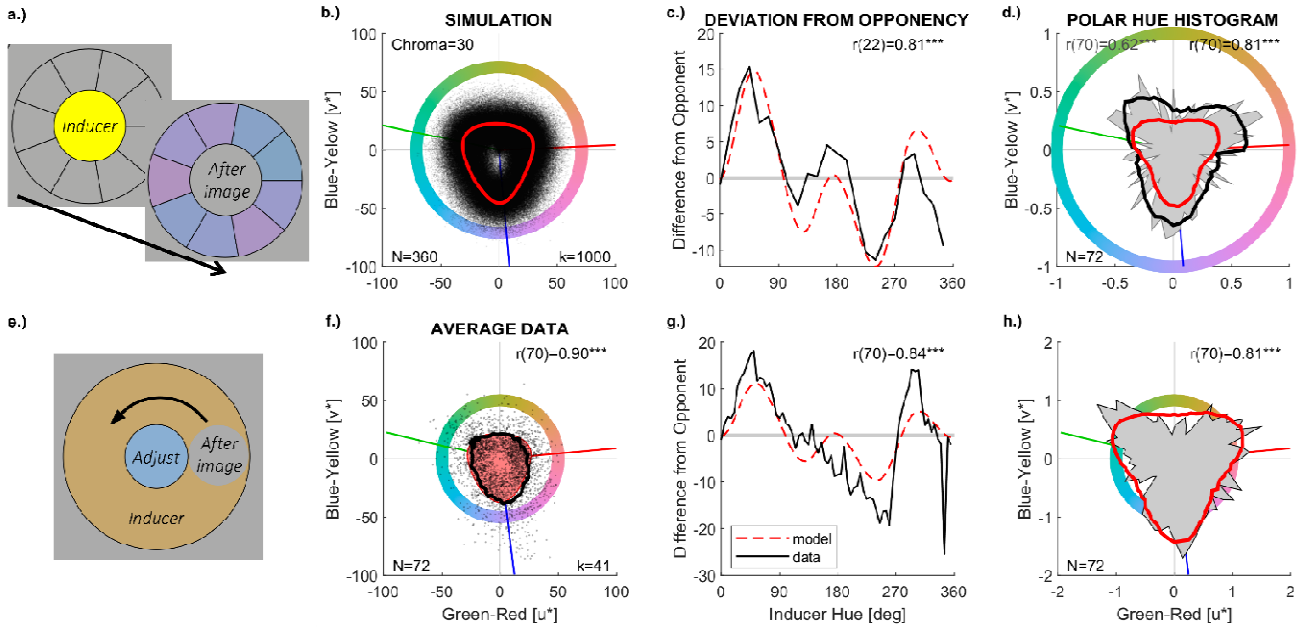

Figure 1. Tasks and Results. The first column (a,d) illustrates stimulus displays and experimental paradigms. The first row (a-d) provides method, model (b), and results (c-d) for the first paradigm. Observers adapt to the inducer display for 30s (yellow in b). Then the inducer display is replaced by a circle of background grey together with nine comparison colours (purple in b) in a circular arrangement around the grey circle. The grey circle in the centre is perceived as the induced afterimage, and observers select the comparison colour that best matches the colour they see in the centre. Panel b illustrates the results of the cone-contrast model without (red line) and with noise (black dots). Note the difference from a circle that would result when afterimages were cone-opponent. The curves in the third column illustrate the deviation of the cone-adaptation model (dashed red curve) and of the measured afterimages (black curve) from the colours opponent to the inducers. The correlation reflects the high similarity in profile of the two curves. The polar histograms in the last column (d,h) counts hue responses (azimuth in panel f) and displays the resulting frequencies as a function of azimuth in a polar plot. The histogram of the measurements is shown by the grey area in the background, the smoothened version of that histogram by the black line, and the red line the histogram of the simulated afterimages. Correlations between simulated and measured afterimage hues are shown at the top of the diagrams. The second row (e-h) corresponds to the chaser-like paradigm. In panel e, the chromatic ring is the inducer. Participants fixated the centre, and the moving, grey circle on the ring produces the afterimage. Observers adjusted hue and chroma of the centre circle to match the moving one. Average afterimage matches (black curve in f) closely correspond with model predictions (red area in the background), yielding a correlation (top right) between measured and simulated afterimage intensity (i.e., chroma). Polar hue histograms (d, h) feature three clusters that closely correspond with model predictions (red line), hence confirming the results from panels c, f, and g. The attached animated image illustrates the pronounced difference between the afterimage and the cone-opponent hue of the yellowish inducer in panel e: The afterimage (which appears after staring at the centre of several seconds) is much more purple than the cone-opponent colour (which is displayed in the animated illustration when the moving circle is in the bottom-right quarter of the inducing ring).

Discussion

All results of the two different afterimage-inducing paradigms confirm that afterimages do not align with cone

model of cone adaptation. The cone-contrast model explains large parts of the variance in hue (>60% of variance) and chroma (>80%) of afterimages. Naïve observers may produce very noisy measurements depending on how diligently they follow the instructions (SupMat). Nevertheless, almost all the data provide unequivocal evidence for the signature of cone-adaptation. Considering that level of measurement noise, our results suggest that afterimages are fully, or almost fully, determined by cone-bleaching at the first stage of colour processing.

Such afterimage formation can be explained through a time lag between cone bleaching and regeneration[7,27]. The cone-adaptation model used here implements adaptation according to Weber's Law, which is a direct consequence of the proportional decrease of photon catches due to cone bleaching: a given light has a certain probability with which it isomerises molecules of retinal bound to opsin. When retinal molecules already underwent isomerisation due to ongoing stimulation by an inducer, that probability applies to the remaining proportion of retinal molecules, implying that the amount of isomerising retinal molecules is proportional to the available, non-isomerised molecules[24,25]. As a result, the adapted cone response is proportional to the inverse of the molecules bleached (isomerised) by the inducer. This multiplicative inverse relationship with inducer cone excitation produces non-linear effects of cone adaption, resulting in the three peaks of afterimage strength, reflected by afterimage chroma and the three hue clusters. The each one of the three afterimage peaks is not determined by the single most strongly adapted cone, but by the least adapted cone, i.e., the other two most strongly adapted cones: If L- and M-cones are most adapted by inducers, S cones dominate the afterimage; if L- and S-cones are adapted, M-cones dominate the afterimages; and if S- and M-cones are most adapted, L cones dominate the afterimages. Since S-cone sensitivity barely overlaps with M- and L-cone sensitivity, the effect of S-cones on L-M-adapted afterimages is much stronger than the effects of L- or M-cones, which are highly correlated, resulting in a pronounced asymmetry along the cone-opponent S-(L+M) axis (close to v*, cf. Figure 1.b).

Earlier evidence that was taken to undermine the role of cone adaptation[8,9] assumed that cone-bleaching and regeneration would cancel each other over time, assuming a linear relationship of cone-bleaching and pigment regeneration over time. However, this assumption does not hold. The non-linear, multiplicative inverse relationship between cone-excitation and resulting cone-adaptation is also found in the time course of cone bleaching and regeneration[28], and in the time course of chromatic adaptation[29]. So, the observation that different temporal sequences of inducer stimulation produce dissimilar afterimages[8,9] is compatible with our findings.

Other behavioural evidence attempted to establish a cone-opponent origin of afterimages through successful nulling of afterimages in cone-opponent space[10]. However, successful nulling in cone-opponent space works independently of whether the appearance of afterimages follows a straight line due to second-stage, cone-opponent adaptation or a bent curve due to nonlinear adaptation, such as cone adaptation. Our results replicate, extend, and explain observations of three clusters that contradict a cone-opponent origin[14].

Unlike what current textbooks suggest[3-5], colour afterimages are neither determined by cone- nor by Hering-like colour opponency. A cursory look at afterimages may be misleading because afterimages resemble cone-opponency at a very coarse level[26]. This is not due to adaptation of the cone-opponent mechanisms at the second stage of colour processing, but to the adapted colour signal from the first stage being propagated to the second and subsequent stages. This propagation of the afterimage signal also explains the physiological responses of retinal ganglion cells as a function of afterimages[10]. The present experimental paradigms allowed a closer look at the precise colours of negative afterimages and reveal that afterimages are not aligned with cone opponency but are almost fully determined by first-stage adaptation. Little variance of perceived afterimages is left that would support additional adaptation at later, subsequent levels of processing.

Evidence for mid-level (e.g., contours and shape[16,30]) or high-level (e.g., knowledge[18]) effects on afterimage do not necessarily reflect the origin of afterimages. Illusory percepts like afterimages involve perceptual uncertainty due to the absence of a physical stimulus[30]. When a sensory signal is uncertain, the perceptual system integrates other available cues to disambiguate the resulting percept. For example, such cues can be shape, object memory, and prior assumptions, as known from memory colour effects, effects of colour categories, and from priming #theDress[31]. If the reliability of the cues can be quantified, such top-down effects of expectations on colour appearance can be modelled through Bayesian cue integration[32]. Obviously, such effects do not occur in the absence of other cues. Hence, top-down, interference effects may modulate the subjective appearance of afterimages due to uncertainty; but they are not the origin of afterimage formation.

From the present results, it is clear that negative colour afterimages are determined by cone adaptation and can be precisely predicted by a straight-forward cone-contrast model of the first stage of colour processing. Our findings do not only decide over general ideas in a decades-old debate about the origin of negative colour afterimages. They establish a quantitative model that comprehensively explains afterimage formation in detail. It's time to update textbooks.

METHOD

Task 1: Fixed-Location Afterimages

Participants. Fifty-two observers took part (36 women, age: 25.1±4.3years). They were compensated by course credits or €8 per hour. Colour vision deficiencies were excluded with the HRR plates (Hardy, Rand, & Rittler, 1954). The experiment were approved by the ethics committee at the University of Gießen (LEK 2017-0030), and informed consent was obtained from all observers.

Apparatus. Stimuli were presented on an Eizo Color Edge Monitor (36,5 x 27cm) with an AMD Radeon Firepro graphics card with a colour resolution was 10 bit per channel. The CIE1931 xyY chromaticity coordinates and luminance of the monitor primaries were R = (0.6851, 0.3110, 27.1), G = (0.2133, 0.7267, 69.4), and B = (0.1521, 0.0450, 4.7). Gamma was 2.2 for all channels and has been corrected.

Stimuli. Twenty-four inducers were sampled along a hue circle in CIELUV at chroma 71 and equal steps of 15 deg starting at 0 deg (cf. Figure SXXXX). Chroma was chosen to be the highest chroma achievable within monitor gamut for all hue directions. Lightness of inducers, comparison colours, and the achromatic disc in the centre of the test display were the same as the background (L* = 70). The white-point was [0.3304, 0.3526, 101.1]. To determine the comparisons, we computed for each hue the opponent hue in CIELUV space; at isoluminance, these are the same as cone-opponent hues in DKL-space. CIELUV-space was preferred because it better controls for perceived chroma DKL-space[33]. The nine hues of the comparison colours were obtained by adding four hues in 10 deg steps to either direction (low or high azimuth) of the opponent hue. Chroma of all comparison colours was kept constant at 30. This level of chroma was determined through piloting and accounts for the lower saturation of the afterimages as compared to the inducers. Table SXXXX provides detailed colour specifications.

Procedure. In one trial, the inducer display was shown for 20 seconds. During this time, a round fixation dot was blinking at a rate of 1Hz at the center of the screen. Observers were asked to stare at this dot; but to make sure they would, they also completed a cover task. In some trials, the round dot would change, for one blink, into a square dot. Observers had to indicate at the very end of a trial whether such a squared dot occurred in the trial or not.

While seeing the afterimage, observers determined which of the 9 comparisons was the best match. Afterimages tended to melt into segment with the colour that looked closest to the afterimage, making the task rather intuitive. Participants used the mouse to indicate the segment with the matching comparison (Figure 1.a). If they could not see any of the comparison colours in the centre they could also click on the center disk to indicate this (resulting in a missing value). After that response, participants responded to the cover task, and if wrong, had to redo the whole trial at the end. A 10-seconds intertrial display followed by a self-parsed break was used to canceled remaining after images to prevent afterimage interference across trials (see SupMat).

Task 2: Chaser-Like Afterimages

Participants. Ten voluntary participants (6 women), including the author (CW) took part. The experiment was approved by the Ethics Committee at the University of Southampton, ERGO 65442.

Apparatus & Stimuli. Three different experimental set-ups were used and calibrated as explained for Task 1 (see Supplementary Material for details. All measurements were conducted in ambient darkness. 72 inducer colours were sampled in 5-deg steps along an isoluminant hue circle in CIELUV-space at L*=70. Inducer chroma was set to be maximal within the respective monitor gamut, resulting in a chroma of 38 (one participant), 42 (two participants), or 50 (everyone else). Figure 1.e and the attached animated image illustrate the stimulus display.

Procedure. In each trial, participants were asked to fixate the centre of the display until the moving circle reaches maximum colourfulness. Then, they adjusted the hue (left/right) and saturation (up/down) of the centre circle using the cursor keys. During a coarse adjustment, they could continuously change colours; but before confirming the adjusted colour, participants needed to do a fine adjustment (by pressing space). In the fine adjustment, colour change by single steps (in radius or in 1 deg azimuth) with each separate key stroke.

Since the adjustment takes time, observers would see afterimages from the adjusted colour attenuating the chroma of the adjusted colour. Two measures were taken to avoid this: During coarse adjustment, black and white circles (not areas) were extending from the centre of the adjusted disks to its rim. These circles, however, would disappear during fine adjustments. In addition, pressing the control key would turn the centre disk temporarily into grey until key release. Observers were asked to wipe out unwanted afterimages from the adjusted centre disk using that key before confirming the adjustment. So, they would press control, wait and move their eyes until the centre disks looks achromatic. They should then stare at the grey circle until the moving circle reaches maximum chroma. Only then, they should release the key and compare the colour they had previously adjusted with the colour of the moving circle. In that case, the adjusted colour was too saturated due to the overlay of the self-afterimage during the adjustment. So, participants needed to lower chroma. They reiterated this procedure until the chroma did not need adjustment after releasing the control key. Only then, participants confirmed adjustments by pressing enter. As in Task 1, the intertrial period was used to prevent afterimage carry-over across trials.

Inducer colours were split into nine series of eight colours. Within a series, the eight colours differed by 45° azimuth. Different series were defined by different starting points (0, 5, 10…40 degree) so that the series covered all 72 inducers. One block of measurements featured one trial for each of 8 inducer colours in a series. Measurements of each block were repeated up to five times. Blocks of measurements were spread over several days. Prior to measurements, participants were trained with practice blocks in the presence and with the feedback of the experimenter (CW) to make sure they understood handling and its purpose.

Cone-Adaptation Model

We modelled adaptation and cone bleaching at the first stage of colour processing by cone contrasts[34-36]. Cone contrasts (CC) are Weber fractions, calculated as the difference between cone excitations of the stimulus (CE) and cone excitations of the adapting colour (CE0) relative to the cone excitations of the adapting colour: CC = (CE-CE0)/CE0. These cone contrasts model cone bleaching[24,25,37-40]. The reduction of sensitivity at high stimulus intensities can be explained by the reduction of available photopigment due to bleaching. Since bleaching is proportional to intensity of the adapting stimulus, one needs proportionally more stimulation (likelihood of photon catches) for detecting a non-adapted stimulus. In psychophysical experiments, adaptation is typically controlled by the colour of the background. In the case of afterimages and contrast induction, the roles are swapped because we model perception of the achromatic background after local adaptation to the inducer. Hence, CE0 is the cone excitation of the inducer, and CC the one of the background. Cone contrast changes with increasing cone

adaptation CE0 according to a multiplicative inverse function (because CE0 increases in the denominator). Cone contrast is calculated independently for the short- (S), medium- (M), and long-wavelength (L) sensitive cones, resulting in S-cone, M-cone, and L-cone contrasts (SC, MC, and LC). Cone adaptation produces shifts towards the peak cone sensitivities, as illustrated by the three peaks in a hue histogram (Figure 1.b).

Results showed that we cannot assume that adaptation to inducers is complete. As an empirical estimate of the strength of adaptation, we set the adapting chroma for modelling afterimages to the chroma of the comparison colours in the first task, and to the grand average of adjustments for the second task. Even if we assumed complete adaptation to the chroma of inducers, results would be largely the same. However, not surprisingly, correlation coefficients would be slightly lower because non-linearities in the model are then higher than in the measurements (see Figure SXXXX and Table SXXXX for details). There is no free parameter in this model.

Acknowledgements

Thanks to Bevil Conway, Kevin O'Regan, and Wendy Adams for helpful comments, and Alexander Nowak for help with data collection. Research was partially funded by the Deutsche Forschungsgemeinschaft (DFG, German Research Foundation) – project number 222641018 – SFB/TRR 135 TP C2, and research funds from the School of Psychology at the University of Southampton.

References

1 Helmholtz, H. L. F. v. *Handbuch der physiologischen Optik*. 1 edn, (Leopold Voss, 1867).

2 Webster, M. A. Visual Adaptation. *Annual review of visual science* **1**, 547-567, doi:10.1146/annurev-vision-082114-035509 (2016).

3 Goldstein, E. B. & Cacciamani, L. *Sensation and perception*. Eleventh edition edn, (Wadsworth, 2021).

4 Wolfe, J. *et al. Sensation and Perception*. 6 edn, (Oxford University Press, 2020).

5 Manzotti, R. A Perception-Based Model of Complementary Afterimages. *SAGE Open* **7**, 2158244016682478, doi:10.1177/2158244016682478 (2017).

6 Horner, D. T. Demonstrations of Color Perception and the Importance of Contours. *Teaching of Psychology* **24**, 267-268, doi:10.1207/s15328023top2404_10 (1997).

7 Brindley, G. S. Two new properties of foveal after-images and a photochemical hypothesis to explain them. *Journal of Physiology (London)* **164**, 168-179, doi:10.1113/jphysiol.1962.sp007011 (1962).

8 Loomis, J. M. The photopigment bleaching hypothesis of complementary after-images: a psychophysical test. *Vision Research* **12**, 1587-1594 (1972).

9 Loomis, J. M. Complementary afterimages and the unequal adapting effects of steady and flickering light*. *Journal of the Optical Society of America* **68**, 411-416, doi:10.1364/JOSA.68.000411 (1978).

10 Zaidi, Q., Ennis, R., Cao, D. & Lee, B. Neural locus of color afterimages. *Current Biology* **22**, 220-224, doi:10.1016/j.cub.2011.12.021 (2012).

11 Hurvich, L. M. & Jameson, D. An opponent-process theory of color vision. *Psychological Review* **64**, 384-404, doi:10.1037/h0041403 (1957).

12 Thompson, P. & Burr, D. Visual aftereffects. *Current Biology* **19**, R11-14, doi:S0960-9822(08)01346-8 [pii] 10.1016/j.cub.2008.10.014 (2009).

13 Webster, M. A. & Mollon, J. D. Changes in colour appearance following post-receptoral adaptation. *Nature* **349**, 235-238, doi:10.1038/349235a0 (1991).

14 Koenderink, J., van Doorn, A., Witzel, C. & Gegenfurtner, K. Hues of Color Afterimages. *i-Perception* **11**, 2041669520903553, doi:10.1177/2041669520903553 (2020).

15 Wilson, M. H. & Brocklebank, R. W. Complementary Hues of After-Images. *Journal of the Optical Society of America* **45**, 293-299, doi:10.1364/JOSA.45.000293 (1955).

16 van Lier, R., Vergeer, M. & Anstis, S. Filling-in afterimage colors between the lines. *Current Biology* **19**, R323-324, doi:S0960-9822(09)00811-2 [pii] 10.1016/j.cub.2009.03.010 (2009).

17 Shimojo, S., Kamitani, Y. & Nishida, S. Afterimage of perceptually filled-in surface. *Science* **293**, 1677-1680, doi:10.1126/science.1060161 (2001).

18 Lupyan, G. Object knowledge changes visual appearance: Semantic effects on color afterimages. *Acta Psychologica* **161**, 117-130, doi:10.1016/j.actpsy.2015.08.006 (2015).

19 Tsuchiya, N. & Koch, C. Continuous flash suppression reduces negative afterimages. *Nature Neuroscience* **8**, 1096, doi:10.1038/nn1500 (2005).

20 Dong, B., Holm, L. & Bao, M. Cortical mechanisms for afterimage formation: evidence from interocular grouping. **7**, 41101, doi:10.1038/srep41101 (2017).

21 Zeki, S., Cheadle, S., Pepper, J. & Mylonas, D. The Constancy of Colored After-Images. *Frontiers in Human Neuroscience* **11**, doi:10.3389/fnhum.2017.00229 (2017).

22 Craik, K. J. W. Origin of Visual After-images. *Nature* **145**, 512-512, doi:10.1038/145512a0 (1940).

23 Pöppel, E. Long-range colour-generating interactions across the retina. *Nature* **320**, 523-525, doi:10.1038/320523a0 (1986).

24 Pugh, E. N., Nikonov, S. & Lamb, T. D. Molecular mechanisms of vertebrate photoreceptor light adaptation. *Current Opinion in Neurobiology* **9**, 410-418, doi:https://doi.org/10.1016/S0959-4388(99)80062-2 (1999).

25 Shapley, R. & Enroth-Cugell, C. Visual adaptation and retinal gain controls. *Progress in retinal research* **3**, 263-346 (1984).

26 Kingdom, F. A. A., Touma, S. & Jennings, B. J. Negative afterimages facilitate the detection of real images. *Vision Research* **170**, 25-34, doi:https://doi.org/10.1016/j.visres.2020.03.005 (2020).

27 Rushton, W. A. H. The Ferrier Lecture, 1962 Visual adaptation. *Proceedings of the Royal Society of London. Series B. Biological Sciences* **162**, 20-46, doi:doi:10.1098/rspb.1965.0024 (1965).

28 Rushton, W. A. & Henry, G. H. Bleaching and regeneration of cone pigments in man. *Vision Research* **8**, 617-631 (1968).

29 Rinner, O. & Gegenfurtner, K. R. Time course of chromatic adaptation for color appearance and discrimination. *Vision Research* **40**, 1813-1826, doi:S0042-6989(00)00050-X [pii] (2000).

30 Powell, G., Bompas, A. & Sumner, P. Making the incredible credible: afterimages are modulated by contextual edges more than real stimuli. *Journal of Vision* **12**, doi:12.10.17 [pii]; 10.1167/12.10.17 (2012).

31 Witzel, C. & Gegenfurtner, K. R. Color Perception: Objects, Constancy, and Categories. *Annual Review of Vision Science* **4**, 475-499, doi:10.1146/annurev-vision-091517-034231 (2018).

32 Witzel, C., Olkkonen, M. & Gegenfurtner, K. R. A Bayesian Model of the Memory Colour Effect. *i-Perception* **9**, 2041669518771715, doi:10.1177/2041669518771715 (2018).

33 Witzel, C. & Gegenfurtner, K. R. Are red, yellow, green, and blue perceptual categories? *Vision Research* **151**, 152-163, doi:https://doi.org/10.1016/j.visres.2018.04.002 (2018).

34 Brainard, D. H. in *Human Color Vision* (eds P. K. Kaiser & Robert M. Boynton) 563-579 (Optical Society of America, 1996).

35 Brainard, D. H. & Stockman, A. in *OSA Handbook of Optics* (ed M. Bass) 10.11-10.56 (McGraw-Hill, 2010).

36 Stockman, A. & Brainard, D. H. in *OSA Handbook of Optics* (ed M. Bass) 11.11-11.104 (McGraw-Hill, 2010).

37 Pugh, E. N. & Lamb, T. D. in *Handbook of Biological Physics* Vol. 3 (eds D. G. Stavenga, W. J. DeGrip, & E. N. Pugh) 183-255 (North-Holland, 2000).

38 Burkhardt, D. A. Light adaptation and photopigment bleaching in cone photoreceptors in situ in the retina of the turtle. *Journal of Neuroscience* **14**, 1091-1105 (1994).

39 Burkhardt, D. A. & Gottesman, J. Light adaptation and responses to contrast flashes in cones of the walleye retina. *Vision Research* **27**, 1409-1420, doi:10.1016/0042-6989(87)90151-9 (1987).

40 Whittle, P. Increments and decrements: luminance discrimination. *Vision Research* **26**, 1677-1691, doi:0042-6989(86)90055-6 [pii] (1986).